



ELSEVIER

Contents lists available at ScienceDirect

International Journal of Adhesion & Adhesives

journal homepage: www.elsevier.com/locate/ijadhadh

Laser ablation surface preparation for adhesive bonding of carbon fiber reinforced epoxy composites



Frank L. Palmieri^{a,*}, Marcus A. Belcher^b, Christopher J. Wohl^a, Kay Y. Blohowiak^b, John W. Connell^a

^a NASA Langley Research Center, MS226, Hampton, VA 23681-2199, USA

^b The Boeing Company, Seattle, WA 98124-2207, USA

ARTICLE INFO

Article history:

Accepted 10 February 2016

Available online 20 February 2016

Keywords:

Lap-shear

Aging

Durability

Failure mode

Nd:YAG pretreatment

ABSTRACT

Adhesive bonding of carbon fiber reinforced plastic (CFRP) epoxy composites provides many advantages over mechanical fastening for assembling aerospace structures including weight savings, reduced manufacturing flow, and added structural efficiency. To ensure the reliability of bonded joints in primary airframe structures, the surface preparation method and execution are critical. Surface preparation is widely recognized as a key step in the bonding process and is one element of a bonding method that must be controlled to produce robust and predictable bonds in a precise and repeatable manner. Laser ablation of composite surface resin can provide an efficient, precise, and reproducible means of preparing composite surfaces for adhesive bonding. Advantages include elimination of physical waste (i.e., grit media and sacrificial peel ply layers that ultimately require disposal), reduction in process variability due to increased precision (e.g. monitoring laser parameters), and automation of surface preparation. This paper describes a surface preparation technique using a nanosecond, frequency-tripled Nd:YAG laser source. Lap shear specimens were laser treated and tested and apparent shear strength and failure modes of lap shear specimens were used to assess mechanical performance over a three-year accelerated aging study by exposing bonded specimens to 71 °C (160 °F) and 85% relative humidity.

Published by Elsevier Ltd.

1. Introduction

There are currently efforts among aircraft manufacturers to advance adhesive bonding technologies to improve airframe design and simplify fabrication methods while simultaneously increasing aircraft performance. These areas of emphasis include integrating bond process controls, real-time, in-line quality control characterization methodologies, and non-destructive assessment of bond strength and quality [1–3]. As part of a continued effort to improve the robustness and efficiency of the surface preparation process for composite-to-composite bonding, the use of laser ablation has been evaluated [4]. In this work, a nanosecond, frequency-tripled Nd:YAG laser has been used to controllably and selectively remove several microns of resin and contaminants from the surface of a composite without damaging the reinforcing fibers. This technique enables application of a precise amount of laser radiation to be imparted onto the surface providing a high degree of control and reproducibility of the surface topography and chemistry. Laser surface treatment can be rapid (up to

approximately 1 m²/min), lending itself to scale-up and automation, and can be practical for use in a variety of settings such as an industrial production facility or repair depot [5,6]. Laser ablation may ultimately be able to replace the use of peel plies and grit blasting surface preparation techniques, both of which create waste byproducts and are difficult to automate. The laser technique has also shown promise for metals, such as titanium and aluminum, with the potential to replace one or more environmentally unfriendly immersion-based chemical treatment steps currently in use [7].

Surface preparation is acknowledged as a critical aspect of bonding because it removes contaminants that may be present during the composite fabrication process (i.e., mold release agents, release plies, and fabrics) and it affects the final texture and chemistry at the interface [2]. Historically, failures of an adhesive bond have often been traced to defects at the bond interface [8,9]. FAA certification methodology for primary bonded airframe structure consistently calls for strict in-process control and post bond inspections [2] to validate the quality of the bond.

One of the state-of-the-art surface treatments for composites is the use of specific peel ply materials, which are applied to the uncured prepreg surface, cured with the part, and then removed immediately prior to application of the adhesive. These peel ply

* Corresponding author. Tel.: +1 757 864 8802.

E-mail address: frank.l.palmieri@nasa.gov (F.L. Palmieri).

surface preparations can provide excellent performance in bonded structures, but must be carefully selected to provide compatibility with the bonded system (substrate, adhesive, process method). Other standard methods include mechanical abrasion, which can provide acceptable performance but may be difficult to automate over large areas [10].

Emergent techniques such as atmospheric pressure plasma, arc discharge, and laser ablation have been demonstrated to be feasible as prebond surface preparation techniques and are rapidly being advanced by the aerospace industry [10–13]. Atmospheric pressure plasmas have shown significant promise for composite surface treatment and are being used in production of automotive and aerospace parts. Depending on scan rate, atmospheric pressure plasmas generally only penetrate into the top few nanometers of a surface and thus are of use if the contamination layer does not exceed this thickness. These plasma techniques can also be used in conjunction with another method, such as peel ply or abrasion to improve the robustness of the surface preparation process. Laser ablation is a subtractive process that relies on laser radiation to remove material from a surface [14–17]. Ultra-violet laser systems are commonly used for high precision work such as medical procedures, machining of fine parts, and printing micro-electronic circuit patterns. The ablation process has been demonstrated to generate precise surface topography concomitant with the removal of surface contaminants and modification of surface chemistry [4,18]. Laser ablation can also selectively etch resin without damaging reinforcing fibers unlike mechanical abrasion which is generally not selective [19]. Depending on part complexity and composite fabrication process, which among other things can control resin surface layer thickness and degree and type of contaminant, plasma and laser surface treatments provide complementary approaches giving users options, depending on their specific manufacturing constraints.

In this study, composite lap shear specimens were fabricated from T800H/3900-2 prepreg, laser ablated using a nanosecond, frequency-tripled, Nd:YAG laser, and then bonded using AF 555M structural adhesive film. Specimens were placed in an environmental chamber at 71 °C (160 °F) and 85% relative humidity (RH) and removed periodically to measure apparent shear strengths and determine failure modes. These results were compared to specimens tested prior to aging and control specimens that were aged in a desiccator. Comparisons were made with specimens that were aged under slightly different conditions and fabricated from the same materials using a peel ply surface treatment [20,21].

2. Experimental

2.1. Materials

Composite panels (carbon fiber reinforced plastic (CFRP), 30.5 cm × 30.5 cm) were fabricated in a vacuum press from 16 plies of unidirectional Torayca P2302-19 prepreg (T800H/3900-2 carbon fiber-toughened epoxy resin system). The panels were cured by placing the prepreg laminate in a stainless steel mold and heating under vacuum at 690 kPa (100 psi). The mold was lined with a high temperature polyimide film in order to produce a smooth surface. The cured laminates were trimmed around the edges and cut into two panels that were each 10.2 cm × 20.3 cm. Scotch-Weld AF 555M structural adhesive film (areal weight: 244 g/m²; 3M Company) was used as received.

2.2. Laser ablation

Laser etching of CFRP panels (10.2 cm × 20.3 cm) was performed using a PhotoMachining, Inc. laser ablation system with a

Coherent Avia[®] frequency tripled Nd:YAG laser (2-watt nominal output at 355 nm and a 10 ns pulse width). The following parameters could be adjusted: laser power, frequency, beam width, beam spacing, scan speed, and number of passes. Prior to bonding, composite surfaces were laser ablated in a crosshatch pattern with 51- μ m line spacing. Laser settings were selected to remove 1–10 μ m of surface resin without damaging underlying carbon fibers, as assessed by optical and electron microscopy of ablated surfaces. The laser was operated at 80% current, 80 kHz frequency, 25.4 cm/s, with 1 pass, and a beam width of 25 μ m. A thermopile type laser power meter was used to measure the laser beam power at the substrate surface and beam power was adjusted to 1 W using thermal lensing effects.

2.3. Microscopy

Material surfaces were imaged using a Zeiss LSM 5 Exciter confocal microscope and an Olympus BH-2 optical microscope equipped with a Hitachi KP-D50 digital color camera.

2.4. Adhesive bonding

After laser ablation, two CFRP panels (10.2 cm × 20.3 cm) were assembled together with a layer of AF 555M adhesive (dimensions: 1.59 cm × 20.3 cm). The adhesive was laid down on one exposed composite panel surface and a roller was applied to manually remove entrapped air. The adhesive was then sandwiched by laying down the second composite panel on top of the previous panel such that there was a 1.27-cm overlap. Shims were used to maintain a uniform bondline thickness of 203 μ m. The assembly was then placed in a vacuum bag and cured in an autoclave at 177 °C (350 °F) and 310 kPa (45 psi) for 2 h. The autoclave operated at a heating rate of 1.1 °C/min and a cooling rate of 6 °C/min. Vacuum (101.6 kPa, 30 in Hg) was applied during the first 30 minutes prior to and during early-stage heating. After the autoclave reached 54 °C (130 °F), the vacuum was turned off for the remaining process cycle.

2.5. Specimen preparation

Bonded panel sets from the autoclave were trimmed to minimize edge effects and subsequently machined into seven 2.54 cm × 19 cm specimens in accordance with ASTM D3165-00 [20]. After all specimens were obtained, quality groups of specimens were selected based on panel origin, void content, and measured bondline thickness to maximize group-to-group uniformity. All specimens were dried in an oven at atmospheric pressure and 50 °C (122 °F) for 24 h followed by heating at 66 °C (150 °F) for an additional 24 h before recording the dry mass for each specimen. Two groups of dried specimens were used to establish baseline apparent shear strength for the unaged specimens by testing at room temperature (RT) and 71 °C (160 °F). The remainder of the specimens was divided into control and experimental lots.

2.6. X-ray computerized tomography (CT)

X-ray CT images of bonded coupons were obtained using a custom imaging system from Hytech, Inc. The X-ray system consists of a micro-focus X-ray source, a flat-panel detector, a rotational stage, and a computer to control data acquisition. The bonded coupons were scanned at 7.6 times magnification resulting in a resolution of 16.7 μ m per voxel.

2.7. Hygrothermal aging

The aging conditions for this study, 71 °C (160 °F) and 85% RH, were selected based on Composite Materials Handbook 17 (CMH-17) for typical assessment of long term durability of a bonded structure [22]. A MicroClimate™ model MCB-1.2 environmental chamber manufactured by Cincinnati Sub-Zero was used. Control specimens were sealed in a plastic bag and stored under low humidity (~20% RH) in desiccators at RT. Control specimens were removed and tested at the same time intervals as those from the aging chamber.

2.8. Mechanical testing and failure mode analysis

Single lap shear specimens (2.54 cm wide with a 1.27 cm overlap) were tested using a slight modification of ASTM D3165-00 with an MTS 810 test frame, MTS 661.20 force transducer (25–100 kN), and MTS 647 hydraulic wedge grips (100 kN capacity; 21-MPa maximum pressure). A minimum of five specimens was tested per set of conditions with the average apparent shear strength reported [23]. Specimens were tested at RT and 71 °C (160 °F). The modification concerning the specimen fabrication method is described in a previous publication [4]. After testing, failure modes were analyzed by visual inspection and categorized in accordance with ASTM D5573-99 and ASTM D5573-ADJ as cohesion (C), thin layer cohesion (TLC), adhesion (A), light fiber tear (LFT), and fiber tear (FT) [24]. For the purposes of discussion in this paper, acceptable failure has been used to capture all failure modes (e.g. C, TLC, LFT and FT) other than adhesion.

3. Results and discussion

3.1. Materials

The composite adherends were fabricated from T800H/3900-2 prepreg as described in the experimental section. After fabrication, all panels were characterized for quality and void content by ultrasonic inspection, microscopic examination, and acid digestion. In general, no significant problems were encountered in panel fabrication and all panels had void contents below 2% by volume.

3.2. Laser ablation

The composite panels were laser ablated across one end of each panel at a width of 1.6 cm, which corresponded to the overlap bond area. The laser was operated at a speed of 25.4 cm/s and 1 pass was used for each line. The laser operating parameters were presented in Section 2.2. A crosshatch pattern was generated as represented in Fig. 1. A variety of patterns and topographical features can be generated or alternatively, the entire surface can be uniformly ablated. The pattern and laser operational parameters selected for this study were based on prior work [4].

Approximately 40 composite panels were laser ablated over multiple weeks to produce 138 individual lap shear specimens

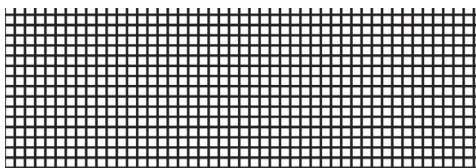


Fig. 1. Illustration of the crosshatch pattern generated on the bonding surfaces of the CFRP substrates.

needed for the three-year aging study. During this time, the laser ablation system underwent some repairs with several parts being replaced, including the f-theta lens, the final optical element. As a consequence, some laser ablated panels differed slightly from others in terms of ablation depth and surface morphology, particularly those fabricated first in the series. There were some inconsistencies observed as variations in color, particularly in the middle of the panels, but the panels were used as-is with no further processing. The color variation was linked to changes in ablation depth caused by laser power variation across the ablation field. From these “first generation” laser ablated panels, 42 lap shear specimens were produced. The heritage of each lap shear specimen was tracked in terms of the specific composite panel from which it was fabricated as well as the complete history of the composite panels, including the specific prepreg batch. One lesson learned from this work was that the ability to measure the energy delivered by the laser at the substrate surface was an effective means of quality control. A device for performing this measurement was integrated into the laser ablation process about half way through the panel fabrication (i.e., after the first generation panels were laser ablated).

3.3. Microscopy

After laser ablation, panels were characterized using optical and confocal microscopy to measure dimensional features created by the laser. A representative confocal microscope image is shown in Fig. 2. Under the laser conditions used for this work, the dimensional features of the “pillars” were on the order of 10–12 μm high, 23–25 μm wide, and 50 μm spacing. The surface striations at the base of the resin pillars are partially exposed carbon fibers. The ability to reproduce these features from panel to panel was excellent provided the energy delivered by the laser at the substrate surface was kept constant.

3.4. Adhesive bonding

Although there were no significant problems observed in the bonding process, some minor variations in bondline thickness were experienced. Bondlines were measured using an optical microscope to view the cross-section of each bond and also calculated from the CT imaging data. These measurement techniques yielded different thicknesses but the scatter within any one technique was reasonable. For example, via CT imaging the bondline thickness averaged 0.16 mm (6.4 mils) with values ranging from 0.14 mm (5.4 mils) to 0.2 mm (7.7 mils). In comparison, the optical microscope gave an average of 0.11 mm (4.3 mils) with a range from 0.08 mm (3.3 mils) to 0.16 mm (6.3 mils). Average void content within adhesive bondlines was 5.7% as determined by CT imaging. The concentration of bondline porosity appeared to only marginally reduce the apparent shear strength (Section 3.8) of the test specimens based on the correlation coefficient of –0.24.

3.5. Specimen randomization

Lots consisting of five or six specimens were randomized in terms of parent composite panels and void content. Randomization was performed by sorting the specimens according to bondline porosity and then dividing the population into 5 ranges of bondline porosity. Specimens were grouped by selecting one specimen from each range. This method resulted in moderate to weak linear correlation values 0.43 and –0.30, respectively, for bondline porosity with specimen age and bondline thickness.

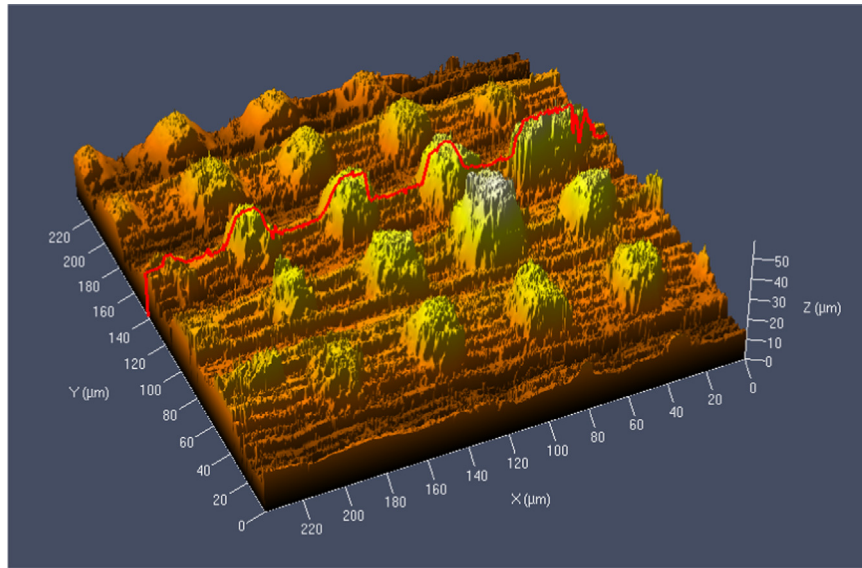


Fig. 2. Confocal microscope image of laser ablated composite surface. The red line indicates where the surface profile is being measured. A feature height of $9.8\ \mu\text{m}$ was observed. (For interpretation of the references to color in this figure legend, the reader is referred to the web version of this article.)

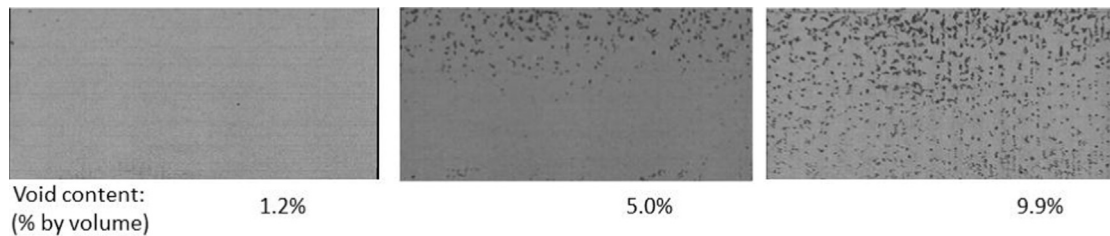


Fig. 3. Representative radiographs of lap shear specimen bond areas.

3.6. X-ray computerized tomography

X-ray radiographs were generated by extracting the bondline from CT images of the coupons and displaying the average intensity as an image. Voids in the image appeared as darker areas and darker shades corresponded to voids occupying more of the bondline thickness. Bondline thickness and total void fraction in the bond line were determined from the difference in image amplitude between the bond-coupon interface and the bond-void interface. Representative radiographs are presented in Fig. 3 for bondlines with 1.2, 5.0 and 9.9% void contents. The radiographs were also analyzed to determine the average bondline thickness of each specimen.

3.7. Hygrothermal aging

To conduct the three-year aging study, a total of 138 single lap shear specimens were tested. The specimens were aged at $71\ ^\circ\text{C}$ ($160\ ^\circ\text{F}$) and 85% RH while control specimens were stored in a low humidity chamber (20% RH) at RT. The temperature and humidity were monitored using a portable data logger that allowed the data to be stored and downloaded to a computer via a USB interface.

3.8. Mechanical testing and failure mode analysis

Prior to beginning the hygrothermal aging process, lap shear testing was conducted on unaged specimens at both RT and $71\ ^\circ\text{C}$ ($160\ ^\circ\text{F}$). The average apparent shear strengths were 35.4 ± 1.7 and 33.4 ± 1.8 MPa, respectively, with nearly 100% cohesion failure. In comparison with a previous study, lap shear specimens

fabricated from the same materials using a wet peel ply surface treatment (Hysol EA-9895) exhibited apparent shear strengths of 37.8 ± 2.7 MPa at RT and 30.4 ± 2.0 MPa at $82\ ^\circ\text{C}$ ($180\ ^\circ\text{F}$) [21]. Although the aging kinetics of the peel-ply samples at $82\ ^\circ\text{C}$ may be faster than the laser ablated specimens aged at $71\ ^\circ\text{C}$, the aging mechanisms are probably similar. The unaged lap shear strengths and failure modes for the two different surface treatments were statistically similar. Aged samples were removed at about 100, 184, 272, 360, 544, 735, 910, and 1095 days. Control (not hygrothermally aged) specimens were also removed from the dessicator and tested, but at less frequent intervals. No significant variation in apparent shear strength value or failure mode was observed for control specimens stored up to three-years. The hygrothermally aged, laser-treated specimens were weighed immediately and mechanically tested within 8 hours of removal from the chamber to minimize drying. The weight of the specimens increased by nearly 0.65% within the initial 100 day interval. The specimens continued to absorb moisture until 544 days of aging when the weight gain approached an asymptotical value at about 0.85%. Control samples exhibited little to no weight change over the three-year test period. The apparent shear strength, void content, and bondline thickness values obtained from specimens at the end of about 1095 days of aging are presented in Table 1. The large variation in void content is due to randomization of this variable within each test group. It is notable that the void content in the bondline of up to 10% did not appear to effect the apparent shear strength. Bondline thickness also appeared to be relatively independent of apparent shear strength over the range of values tested.

Table 1

Apparent shear strength and bondline properties comparing specimens with approximately 1095 days of accelerated aging with control specimens. Because of time constraints (especially for elevated temperature testing) not all samples were tested on the same day. Specimens were held in the aging chamber until the day of testing. The uncertainty shown is one standard deviation.

Aging/test conditions	Apparent shear strength (MPa)	Void (%)	Bondline thickness (μm)
Aged 1099 days at 71 °C and 85% RH, tested at RT	22.5 ± 4.0	6.3 ± 4.1	155 ± 15.0
Aged 1095 days at 71 °C and 85% RH, test at 71 °C	19.4 ± 0.9	7.2 ± 3.3	163 ± 13.2
Control: Aged 1092 days at RT and 15% RH, tested at RT	36.3 ± 2.7	6.5 ± 3.4	154 ± 5.3
Control: Aged 1093 days at RT and 15% RH, tested at 71 °C	31.3 ± 1.1	5.9 ± 3.0	158 ± 17.2

After 1095 days of aging, the apparent shear strength was 22.5 ± 4.0 MPa whereas the control specimens exhibited a value of 36.3 MPa ± 2.7 MPa. This represents a retention in apparent shear strength of about 62% while nearly 100% cohesion type failure was maintained for both the aged and control specimens. In comparison to the previous study with aging conducted at 82 °C (180 °F) and 85% RH using lap shear specimens fabricated with wet peel ply surface treatment, after 772 days aging the apparent shear strength was 24.4 ± 2.9 MPa (65% retention) with predominantly cohesion failures observed [21]. The similarity of the results from these two tests is notable despite the difference in aging temperatures.

The apparent shear strength values for control and aged specimens obtained at 71 °C (160 °F) after 1095 days aging are presented in Table 1. After 1095 days of aging and testing at 71 °C (160 °F), the apparent shear strengths averaged 31.3 ± 1.1 MPa for the control specimens and 19.4 ± 0.9 MPa for the aged specimens. Retention of apparent shear strength was 62% while nearly 100% cohesion failure was observed in both the aged and control specimens. In comparison to the 82 °C (180 °F)/85% RH data from the same materials using a wet peel ply surface treatment, after 772 days aging the apparent shear strength when tested at 82 °C (180 °F) was 31.6 ± 2.6 MPa for the control specimens and 21.4 ± 2.5 MPa for the aged specimens with predominantly cohesion failures observed [21]. Retention of apparent shear strength was about 67%.

Detailed investigation of the failure modes revealed that specimens from the first generation laser processes exhibited the largest decrease in cohesion type failure modes. In some cases, specimens from the first generation laser process resulted in less than 10% acceptable failure mode while specimens from the second generation laser process exhibited greater than 90%. All of the specimens that exhibited low cohesion type failures also had the lowest apparent shear strengths within their respective sample set. The heritage of all specimens that exhibited adhesion failure was traced through their fabrication steps and it was determined that they were part of the first generation of laser ablated panels. Thus, the laser processing conditions are directly linked to the loss of mechanical properties observed after hygrothermal aging. Because the reduced bond properties were isolated to specimens produced using the first generation laser process (i.e., when the laser was not operating properly), these specimens were removed from the data set as outliers.

Three-years of aging data are presented graphically in Figs. 4 and 5 for specimens tested at RT and at 71 °C (160 °F), respectively. By removing the specimens from the first generation laser process, trends in bond performance can be observed with

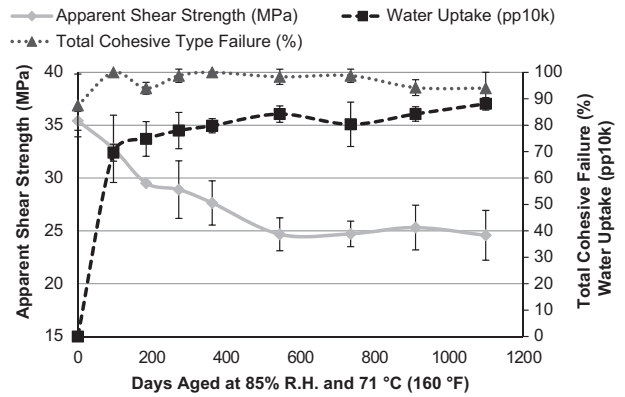


Fig. 4. Apparent shear strength at RT, water uptake, and percent cohesion failure as a function of hygrothermal aging time. First generation specimens were excluded from the data set.

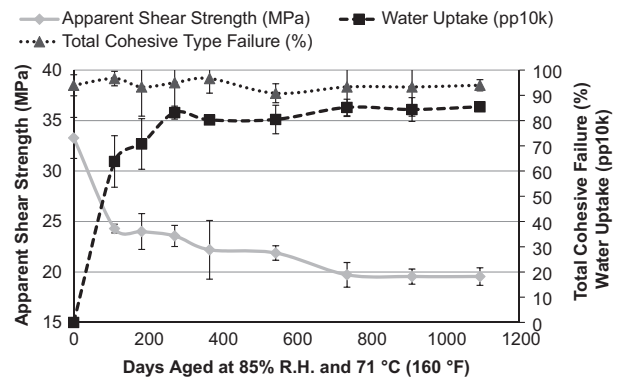


Fig. 5. Apparent shear strength at 71 °C (160 °F), water uptake, and percent cohesion failure as a function of hygrothermal aging time. First generation specimens were excluded from the data set.

specimen age. Included in Figs. 4 and 5 are apparent shear strength, water uptake, and failure mode. The water content of the specimens increased rapidly in the first 200 days of aging and then plateaued at about 500 days. The average water uptake for aged lap shear specimens was about 0.80%. The change in apparent shear strength followed a very similar trend. The steepest decrease in apparent shear strength corresponded to the steepest increase in water content. A strong, inverse correlation coefficient between water content and apparent shear strength was calculated to be -0.73. Failure mode, however, did not follow the same trend. The acceptable failure mode presented in these data is a combined statistic that includes cohesion failure, thin layer cohesion failure, fiber tear, and light fiber tear. For hygrothermally aged specimens, the amount of acceptable failure decreased slightly after 200 days and remained at approximately 90%. Although it is not presented in the data, the acceptable failure mode changed from predominantly cohesion failure in the adhesive to light fiber tear and eventually developed into fiber tear. This suggests that the adhesive/adherend interface did not degrade during the aging process, but moisture absorption into the adherend resulted in reduced apparent shear strengths.

Further analysis of all lap shear specimens fabricated from first generation panels showed some interesting trends. Of the 42 first generation specimens, those in the unaged and control lots did not exhibit any adhesion failures and the apparent shear strengths were comparable to the rest of the samples within their respective batch. As previously described, first generation laser ablated specimens that underwent hygrothermal aging exhibited statistically lower apparent shear strengths within their respective batches and began to exhibit adhesion failures after around 200 days of aging. Specimens from all

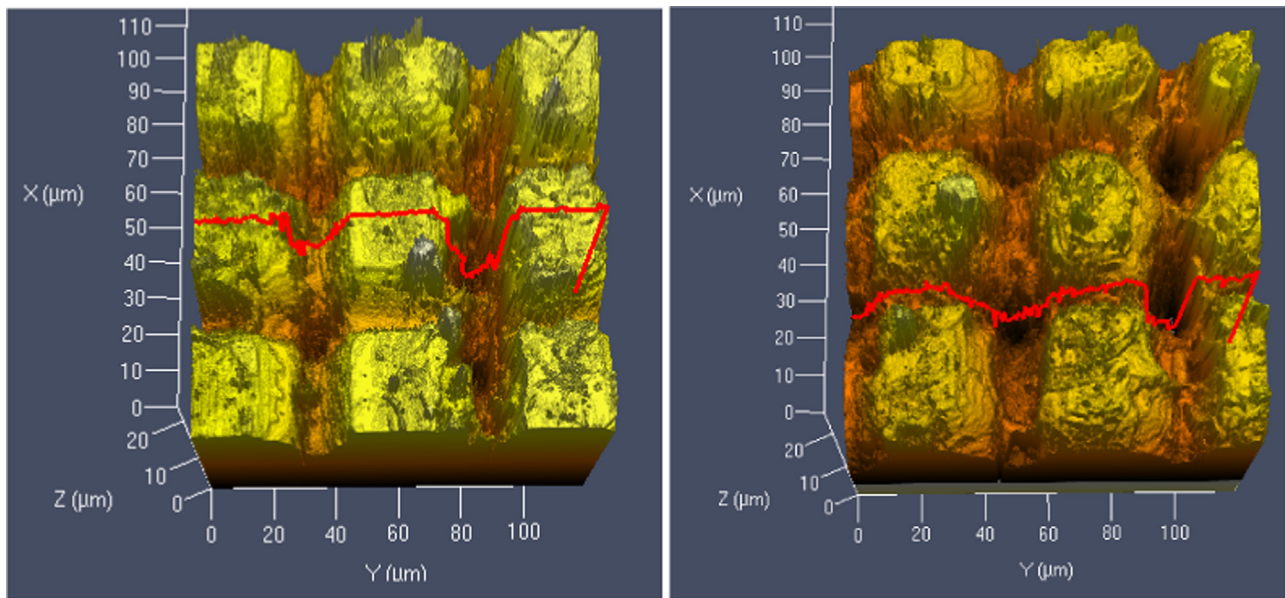


Fig. 6. Confocal microscope image of laser ablated composite surface. Lower laser power results in less ablation depth and surface coverage (left) compared to higher power (right).

subsequent laser processing generations exhibited predominantly acceptable failure modes and high apparent shear strengths. This suggests that the first generation laser ablated panels did not receive uniform surface treatment over the entire bond area due to improper function of the laser. Fig. 6 shows confocal microscope images of surfaces ablated at different laser powers consistent with specimens ablated with first and second laser generations. Low power ablation at the raster speeds and parameters selected leaves unablated surface and removes less material than surfaces ablated at higher powers. It is believed that unablated and under ablated surfaces led to incomplete surface preparation and poor bond performance in first generation specimens.

Although the difference in surface treatment for the first generation specimens was evident in the reduction in ablation depth and coverage, the effect on mechanical properties and failure mode was not apparent until after hygrothermal aging for at least 200 days. This observation further emphasizes the importance of continuously monitoring the laser pulse energy at the substrate surface to ensure consistent ablation as well as the importance of process control for surface preparation of adhesively bonded joints. As a result of this work, protocols were developed to better verify that the laser ablation process was being conducted in a repeatable, traceable manner so that any malfunction of the laser could be readily detected.

4. Conclusions

A 355-nm, nanosecond pulsed Nd:YAG laser was used to ablate patterns into the surface of CFRP adherends to a depth of around 10–12 μm without damaging carbon fibers. The adherends were characterized via microscopy and subsequently used to fabricate single lap shear specimens using AF 555M adhesive. The single lap shear specimens were hygrothermally aged at 71 $^{\circ}\text{C}$ (160 $^{\circ}\text{F}$) and 85% RH for three-years. The reduction in apparent shear strength correlated well with increasing water uptake. Trends in failure mode indicated that aging did not significantly degrade the laser treated interface, and that reduced mechanical properties likely stemmed from water absorption into the composite adherends. Adhesion failure in a subset of aged specimens was traced back to a laser malfunction during surface treatment, which left a

significant portion of the faying surface with either reduced or no ablation. It was found that measuring laser pulse energy at the substrate provided an effective means of quality control for the preparation of highly uniform faying surfaces. Overall, the hygrothermal stability of laser ablated CFRP performed similarly to the same substrates prepared with a wet peel ply surface treatment [21]. The advantage of laser ablation as a pre-bonding treatment is that it can provide a precise and reproducible surface preparation that is amenable to scale-up leading to improved reproducibility and robustness in a production environment.

Acknowledgments

The authors thank the following personnel from NASA Langley Research Center (LaRC): John W. Hopkins of for conducting the laser ablation surface treatment; Hoa Luong, Sean Britton, Richard Chattin, Louis Simmons, and Ed Townsley for laminate fabrication, bonded specimen fabrication, specimen preparation, and lap shear testing; and Raymond Parker for X-ray CT data collection and analysis.

References

- [1] Piehl MJ, Bossi RH, Blohowiak KY, Dilligan MA, Grace WB. Efficient certification of bonded primary structure. In: Proceedings of the 2013 SAMPE conference. Long Beach, CA; May 6–9, 2013.
- [2] Bossi R, Piehl M. Bonding primary aircraft structure: the issues. *Manuf Eng* 2011;101–9.
- [3] Pertont M, Blouin A, Monchalain J-P. Adhesive bond testing of carbon-epoxy composites by laser shockwave. *J Phys D: Appl Phys* 2011;44(3):034012.
- [4] Belcher MA, Wohl CJ, Hopkins JW, Connell JW. Laser surface preparation for bonding of aerospace composites. *Eng Comput Mech* 2011;164(3):133–8. <http://dx.doi.org/10.1680/eacm.2011.164.3.133>.
- [5] Fischer F, Kreling S, Gaebler F, Delmdahl R. Using excimer lasers to clean CFRP prior to adhesive bonding. *Reinf Plast* 2013;57(5):43–6.
- [6] Reutzel T. FRC Cherry Point implementation Institute for manufacturing and sustainment technologies newsletter, 1; 2010. p. 1.
- [7] Palmieri FL, Watson KA, Morales G, Williams T, Hicks R, Wohl CJ, Hopkins JW, Connell JW. Laser ablative surface treatment for enhanced bonding of Ti-6Al-4V alloy. *Appl Mater Interfaces* 2012;5(4):1254–61.
- [8] Davis G. Contamination of surfaces: origin, detection and effect on adhesion. *Surf Interface Anal* 1993;20:368–72.

- [9] Davis M, Bond D. Principles and practices of adhesive bonded structural joints and repairs. *Int J Adhes Adhes* 1999;19(2–3):91–105.
- [10] Kanerva M, Saarel O. The peel ply surface treatment for adhesive bonding of composites: a review. *Int J Adhes Adhes* 2013;43:60–9.
- [11] Encinas N, Oakley BR, Belcher MA, Blohowiak KY, Dillingham RG, Abenojar J, Martínez MA. Surface modification of aircraft used composites for adhesive bonding. *Int J Adhes Adhes* 2014;50:157–63.
- [12] Rechner R, Jansen I, Beyer E. Influence on the strength and aging resistance of aluminum joints by laser pre-treatment and surface modification. *Int J Adhes Adhes* 2010;30:595–601.
- [13] Broad R, French J, Sauer J. CLP new, effective, ecological surface pretreatment for highly durable adhesively bonded metal joints. *Int J Adhes Adhes* 1999;19:193–8.
- [14] Molitor P, Barron V, Young T. Surface treatment of titanium for adhesive bonding to polymer composites: a review. *Int J Adhes Adhes* 2001;21:129–36.
- [15] Baburaj E, Starikov D, Evans S, Shafeev G, Bensaoula A. Enhancement of adhesive joint strength by laser surface modification. *Int J Adhes Adhes* 2007;27:268–76.
- [16] Rotel M, Zahavi J, Tamir S, Buchman A, Dodiuk H. Pre-bonding technology based on excimer laser surface treatment. *Appl Surf Sci* 2000;154–155:610–6.
- [17] Benard Q, Fois M, Grisel M, Lauren P. Surface treatment of carbon/epoxy and glass/epoxy composites with an excimer laser beam. *Int J Adhes Adhes* 2006;26(7):543–9.
- [18] Benard Q, Fois M, Grisel M, Laurens P, Joubert F. Influence of the polymer surface layer on the adhesion of polymer matrix composites. *J Thermoplast Compos Mater* 2009;22:51–61.
- [19] Almuhammadi K, Selvakumaran L, Alfani M, Yang Y, Bera TK, Lubineau G. Laser-based surface preparation of composite laminates leads to improved electrodes for electrical measurements. *Appl Surf Sci* 2015;359:388–97.
- [20] Jensen BJ, Lowther SE, Hou TH, Chang AC, Gupta MC, Familant H. Novel surface treatments for bonding composite structure. In: *Proceedings of the 27th Annual Meeting of the Adhesion Society*; 2004. p. 323–5.
- [21] Knight G, Hou TH, Belcher MA, Palmieri FL, Wohl CJ, Connell JW. Hygrothermal aging of composite single lap shear specimens comprised of AF-555M adhesive and T800/3900-2 adherends. *Int J Adhes Adhes* 2012;39:1–7.
- [22] *Composite Materials Handbook 17 (CMH-17)*. MIL-HDBK-17-1F, vol. 1 Section 2.2.7 2.2.7 moisture absorption and conditioning factors, Department of Defense handbook; June, 2002.
- [23] ASTM D3165 – 00. Standard test method for strength properties of adhesives in shear by tension loading of single-lap-joint laminated assemblies.
- [24] ASTM D5573-99 and ASTM D5573-ADJ. Standard practice for classifying failure modes in fiber-reinforced-plastic (FRP) joints.